

Images compression techniques for wireless sensor network applications

Mohsen Nasri · Abdelhamid Helali · Halim Sghaier · Hassen Maaref

Received: 16 November 2013 / Accepted: 24 October 2014 / Published online: 28 November 2014
© Springer Science+Business Media New York 2014

Abstract Adaptive compression for images transmission in resource-constrained multi-hop wireless network applications is considered. In this strategy, development of an energy efficient image compression scheme is proposed as a means to overcome the computation and/or energy limitation of individual nodes. It has the additional benefit of extending the “life” of individual node by saving its energy power. Two methods for energy efficient image compression are proposed and investigated with respect to energy consumption and image quality. Simulation results show that the proposed scheme prolongs the system lifetime and minimizes the computation energy by reducing the number of arithmetic operations and memory accesses.

Keywords Adaptive compression · Image transmission · Energy conservation · Wireless sensor networks

1 Introduction

Recently wireless sensor network (WSN) has become one of the basic networking technologies since it can be deployed without communication infrastructures [Mohamed El-Semary](#)

M. Nasri (✉) · A. Helali · H. Sghaier · H. Maaref
Laboratory of Micro-Optoelectronics and Nanostructures (LMON),
Sciences Faculty of Monastir, 5019 Monastir, Tunisia
e-mail: mohsen12_nasri@yahoo.fr

A. Helali
e-mail: abdelhamid.helali@isimm.rnu.tn

H. Sghaier
e-mail: halim.sghaier@isimm.rnu.tn

H. Maaref
e-mail: hassen.maaref@fsm.rnu.tn

M. Nasri
College of Computer and Information Sciences, Majmaah University,
Al Majmaah, Saudi Arabia

and [Mostafa Abdel-Azim \(2013\)](#). WSNs are being deployed in a wide range of potential applications scenarios, including forest monitoring, military surveillance, object tracking, traffic control, remote medical systems, and industrial applications [Flammini et al. \(2009\)](#). Such networks are based on small sensor nodes and a sink as depicted in Fig. 1. A typical sensor node consists of four main components: (i) a sensing unit including one or more sensors and an analog-to-digital converters for data acquisition; (ii) a data processor including a micro-controller and a memory for local data processing; (iii) a radio sub-system (RF unit) in order to transmit the data over a wireless channel to a designated sink; and (iv) a power source. Depending on the specific application, sensor nodes may also include additional components which are optional such as a location finding system to determine their position, a mobilizer to change their location or configuration.

For wireless multimedia network, sensor nodes are equipped with multimedia devices such as cameras. These devices are smaller, and offer more performances in terms of speed and image quality. Thus such network will have the capability to transmit multimedia data. The most important requirements of image transmission in WSNs are: Image sensing, allocated memory and image processing.

Despite the advantages of wireless sensor network applications, the wireless sensor nodes are limited energy, storage capacity, computation capability, and communication range. Given the stringent resource, WSNs present strong limits for the image transfer because the image based applications represent visual data requires a large amount of information, which in turn leads to high data rate. Therefore, approaches to optimize data transmission and increase network lifetime are useful.

To address the above mentioned concerns, the image transmission optimization through WSNs is mainly done by the implementation of a distributed image compression embed-

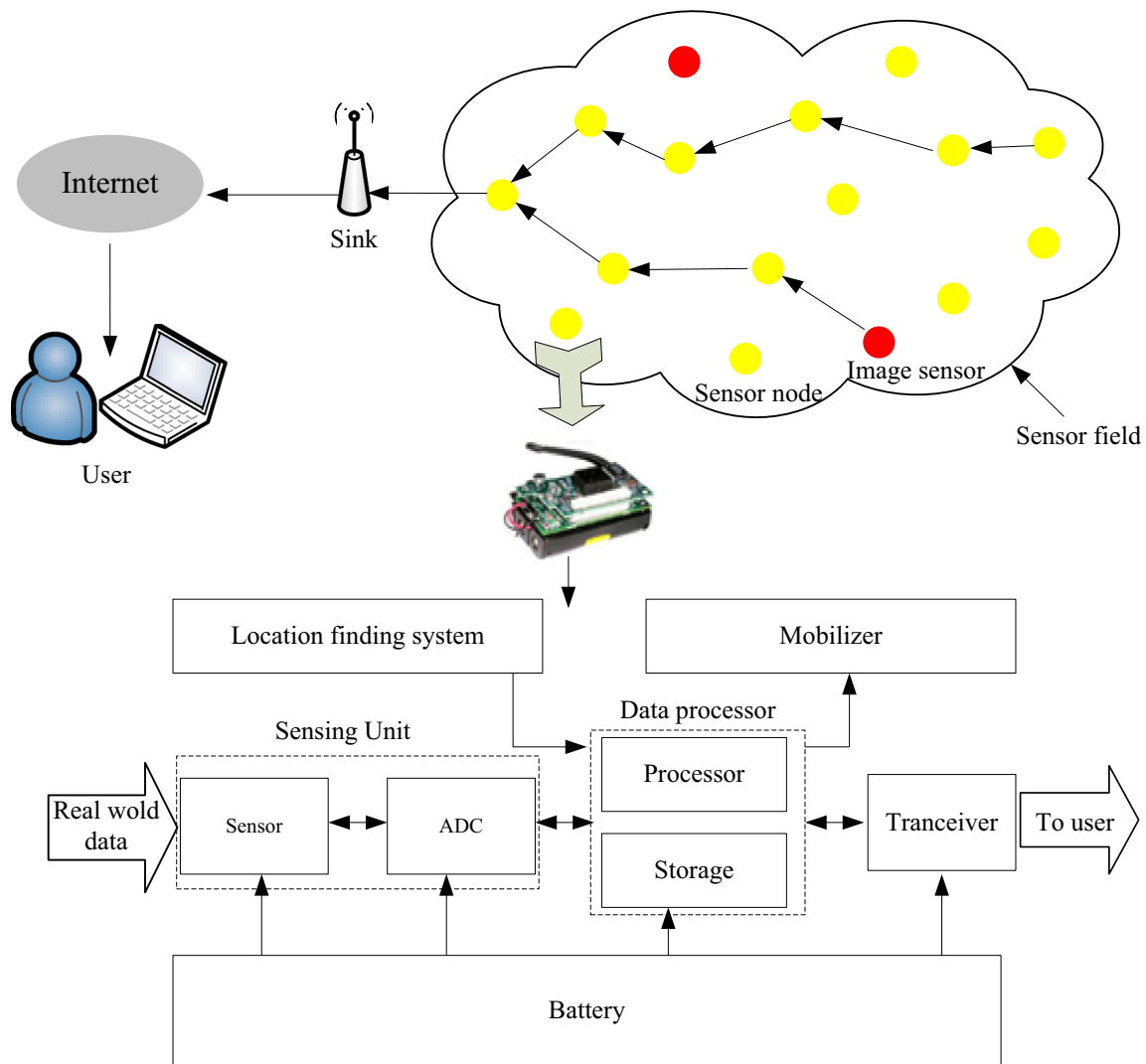


Fig. 1 Sensor network architecture

ded algorithm in order to reduce the number of transmitted bits, thus reducing the energy consumption. This technique is based on the fact that an individual node does not have a sufficient computational power to completely compress a large volume of data to meet the application requirements; this is not possible unless the node distributes the computational task among other nodes. In this case, a distributed method to share the processing task is necessary. In this paper, we propose an alternative image transmission approach in WSNs, based on JPEG2000 image compression standard using Matlab and C from Jasper. JPEG2000 can provide various new additional functions such as high resolutions image compression, progressive transmission and scalable image coding. This approach is based on discrete wavelet transform (DWT) and embedded block coding with optimized truncation (EBCOT) which uses a better order of transmission.

This paper is organized as follows: In the next two sections we summarize related work and describes transmis-

sion scheme in WSNs. Results and discussions are shown in Sect. 4. Finally, Sect. 5 concludes this work.

2 Related work

In typical wireless sensor network applications, the energy consumption is the most critical factor because sensor nodes have a very limited energy supply and are expected to operate independently over a long time-period Liu et al. (2009). For this reason, image transfer presents major challenge which raises issues related to its representation, its storage and its transmission. Therefore, extensive research has focused on how to minimize the energy consumption and prolong the network lifetime Park et al. (2007).

In this case, some research related to wireless sensor is based on energy-efficient routing protocol to reduce power

consumption of a wireless sensors network during image transmission. In [Heinzelman et al. \(2000\)](#), a low energy adaptive clustering hierarchy (LEACH) is considered. Using the purpose, LEACH is able to incorporate data fusion into the routing protocol to reduce the transmitted information quantity being transmitted over the wireless channel. This technique is based on single-hop routing, where the cluster head transmits directly the data to the destination. Due to the limited transmission range of sensor nodes, the adopted protocol appears infeasible in large scale sensor networks. To solve this problem, a multi-hop communication model is proposed in [Heinzelman et al. \(1999\)](#), [Jeon et al. \(2009\)](#). In this model, sensor protocols for information via negotiation (SPIN) efficiently disseminates information in a multi-hop manner is investigated. In the same axis, a routing protocol through a backbone is considered in order to reduce the communication overhead for route discovery and the number of active nodes for WSNs. The main idea of the purpose is to partition the network into different clusters. Each cluster is composed of a cluster head with linked to form the connected backbone and many cluster member nodes [Muthuramalingam et al. \(2008\)](#).

On the other hand, some related issues concern the image transmission over WSNs with an adaptive compression and transmission. In [Ferrigno et al. \(2005\)](#) a platform to evaluate the performance of different traditional algorithms for the image compression in a single sensor node is purposed analyzing five algorithms: joint photographic experts group (JPEG), spread spectrum (SS), discrete cosine transform (DCT), set partitioning in hierarchical trees (SPIHT) and JPEG2000. Research shows that SS is the unique algorithm which presents energy savings with respect to the no-compression case, allowing a power reduction of about 29 %. The mechanism proposed in [Wu and Chen \(2005\)](#) uses a scheme based on an SPIHT coding of data blocks generated from parent–child relationships of wavelet coefficients. This parent–child relationship is performed in order to reinforce SPIHT fragilities in bit error transmission cases. The adopted approach in [Wu and Abouzeid \(2004\)](#) has introduced a power aware technique that incorporates the local compression JPEG2000 standard. They formulated the image transmission problem as an optimization problem and proposed a heuristic algorithm called the minimize total energy (MTE). In [Wagner et al. \(2003\)](#), a distributed image compression for images captured by sensor nodes having overlapping fields of view is considered. The approach uses a technique similar to the stereo-image compression to identify an overlap in the images of neighboring sensor nodes [Boulgouris and Strintzis \(2002\)](#). Distributed image compression using the JPEG2000 standard is proposed in [Wu and Abouzeid \(2005\)](#). Its main idea is based on the distribution of the wavelet transform processing workload between various nodes. Two methods for data exchange have been proposed: The paral-

lel wavelets transform method and the tiling method. In [Lu et al. \(2008\)](#), the distributed implementation scheme of the lapped biorthogonal transform (LBT) based on a clustering architecture overcomes the computation and energy limitation of individual nodes by sharing the tasks processing. This approach is intended to extend the lifetime of the wireless sensor network under a specific image quality requirement.

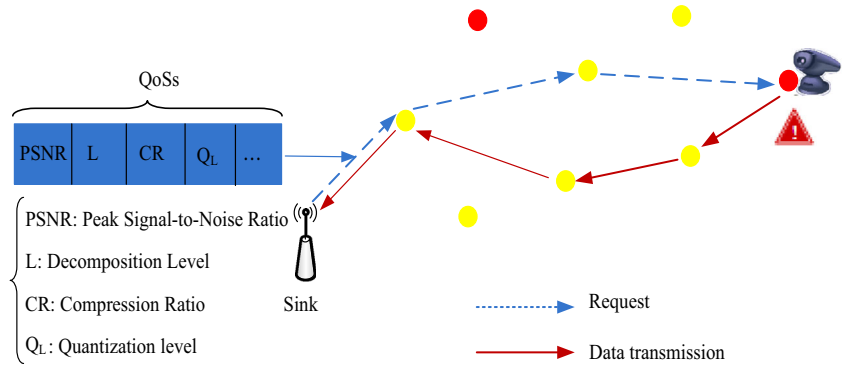
In the same context, we propose a technique to reduce power consumption of wireless sensor network applications during image compression and transmission using the JPEG2000 standard. The purpose is to speed up the compression, optimize the network and to save as much as possible the “life” of individual node by saving its energy power.

3 Transmission scheme in WSNs

Nowadays, more and more multimedia applications integrate wireless transmission functionalities. Due to their ease of deployment, WSNs are being deployed in very diverse multimedia application scenarios. In the context, the main task of a sensor node is to sense the environment and report what happens. Data collected by sensor nodes are usually routed back to a sink node by a multiple-hop communication. Each sensor node has two roles, data gathering and data relaying. In order to make image transmissions possible via energy preservation and allocated memory based heuristic. We use a scenario to request image quality-of-service (QoS) parameters as depicted in [Fig. 2](#).

In this scenario a request specifying the necessary constraints of QoSs is required to initiate image transmission scheme with the operation parameters such as: peak signal-to-noise ratio (PSNR), compression ratio (CR), decomposition level.... When sending an image request, the monitor specifies the desired parameters. The request is initiated by the sink and then conveyed through the intermediate nodes using a multi-hop communication. Each sensor node involved in the transmission request process saves in its memory all the requested parameters. These parameters will be checked during the compression process to determine the number of hops needed from source to sink. This technique makes the number of hops depending on the routing algorithm and the distance from source to sink as well. The scenario is based on image compressing system which supports the rich set of features that are not available in other standards, such as excellent low bit-rate performance, both lossy and lossless encoding in one algorithm, random code stream access, precise single-pass rate control, region-of-interest coding and improved error resiliency. In this investigation, the communication environment is assumed to be contention-free and error-free. In this approach we focus on the problem of efficiently compressing and transmitting images in a resource-constrained multi-hop wireless. We pro-

Fig. 2 Scenario based on the image request



pose a distributed image compression scheme where nodes compress an image while forwarding it to the destination subject to a specific image quality requirement and reduce energy consumption of sensor nodes to prolong lifetime of finite capacity batteries.

3.1 Image processing in WSNs

Due to limited battery lifetime at each sensor, it is obvious that reducing transmitted data will increase energy efficiency and network lifetime. However, the most evident solution is the image compression. The purpose of image compression is to reduce the number of bits required in representing image by removing the spatial and spectral redundancies as much as possible. In this paper, the proposed image transmission scheme is based on wavelet image transform. The structure of a transform coder is illustrated in Fig. 3.

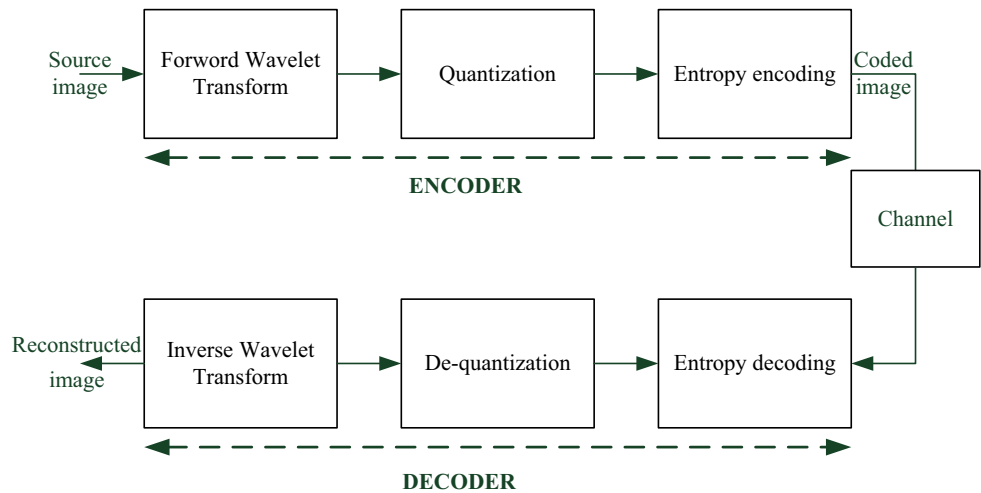
The main objectives achieved by this image compressing system are: progressive transmission, progressive quality, reduced allocated memory, minimized energy consumption, and optimized network lifetime.

More recently, the DWT has gained an efficient tool for signal processing in general and in image compression research in particular. The DWT carries out an analysis of

a signal with localizations in both time and frequency. This is actually a method of multi-resolution which reduces the amount of processed data and therefore would facilitate a progressive image’s transmission. Thus, the wavelet transform is more robust under transmission and decoding errors, and also facilitates progressive transmission of images. Theoretically, DWT is a 2 dimensional separable filtering operation across rows and columns of input image. This is achieved by first applying the low-pass filter (LPF) and a high-pass filter (HPF) to the lines of samples, row by-row, and then re-filtering the output to the columns by the same filters. As a result, the image is divided into 4 sub bands: low-low (LL₁), low- high-low (HL₁), high (LH₁) and high-high (HH₁) as shown in Fig. 4. The high-pass sub-band represents residual information of the original image, needed for the perfect reconstruction of the original set from the low resolution version. Specifically, the LL₁ sub-band can be transformed again to form LL₂, HL₂, LH₂, and HH₂ sub-bands, producing a two-level wavelet transform... and so on.

After the DWT, all the sub-bands are quantized to reduce the precision of the sub-bands and contribute in achieving compression. The quantized DWT coefficients are converted into sign-magnitude represented prior to entropy coding. In the embedded block coding method which is used

Fig. 3 Functional block diagram of JPEG 2000 encoder



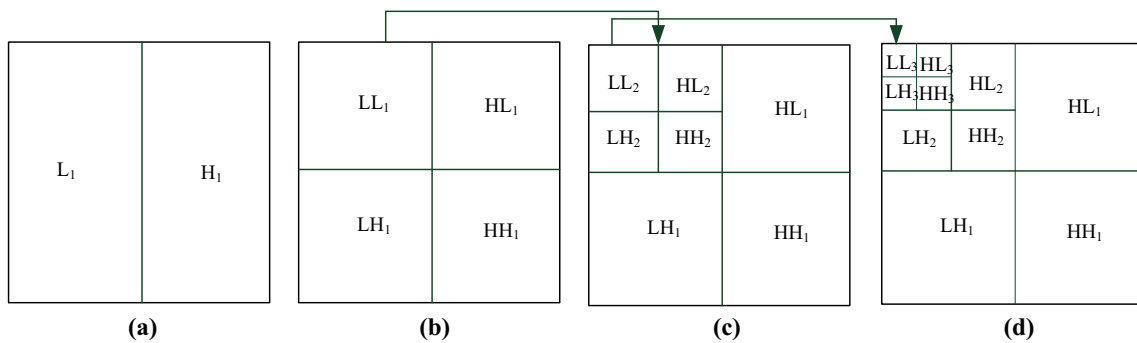


Fig. 4 Illustration of wavelet spectral decomposition. **a** The 1D Wavelet Transform. **b** The first decomposition level. **c** The second decomposition level. **d** The third decomposition level

in JPEG2000 standard, each sub-band (corresponding to LL_i, LH_i, HL_i and HH_i component at each wavelet decomposition level) is divided into small blocks called ‘code blocks’. And then each code block is coded independently from the other ones thus producing an elementary embedded bit-stream. During the coding phase, each code-block is decomposed into a number of bit-planes: One sign bit-plane and several magnitude bit-planes. The entropy coder for JPEG2000 uses embedded block coding with optimal truncation (EBCOT). EBCOT is divided into two coding.

3.2 System model

We consider a multi-hop wireless sensor network that wirelessly interconnected sensor nodes able to retrieve and handle a still image. Their operation can be considered as the convergence between the classical wireless sensor nodes and distributed image sensors. After receiving an image request, every image sensor generates a raw image and transmits it to the sink. When sending an image request, the sink specifies the desired image quality. In the request, the bit rate of a compressed image (q), the wavelet decomposition level, the

PSNR, the quantization level (Q_L) and the CR are specified. For this study, we have adopted the 9/7 wavelet transforms implemented via lifting scheme (LS). This technique calculates the DWT using a spatial domain analysis, and consists of a series of split, predict and update steps that modify, or lift, one set of samples to be used in the next step as shown in Fig. 5. The split step separates odd ($x_o(k)$) and even ($x_e(k)$) samples: $x_e(k) = \{x_{2k}, k \in \mathbb{Z}\}$, $x_o(k) = \{x_{2k+1}, k \in \mathbb{Z}\}$.

The predict step predicts values in the odd set, as follows:

$$P_1 : x_{(2k+1)_{new}} = x_{(2k+1)_{old}} + a \cdot (x_{(2k)_{left}} + x_{(2k)_{right}}) \quad (1)$$

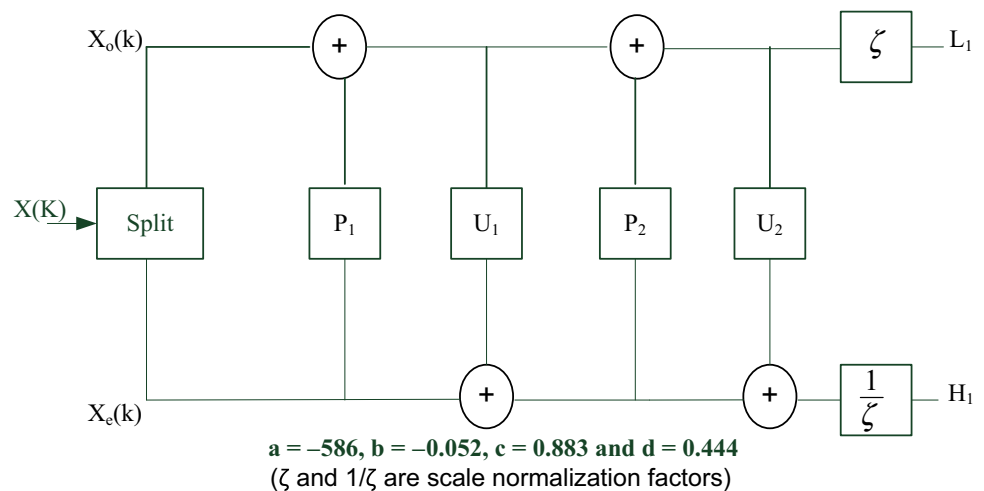
where a is the predict step coefficient. The update step uses the new wavelet coefficients in the odd set to update the even set producing “smooth” or “scaling” coefficients:

$$U_1 : x_{(2k)_{new}} = x_{(2k)_{old}} + b \cdot (x_{(2k+1)_{left}} + x_{(2k+1)_{right}}) \quad (2)$$

where b is the update step coefficient.

The results, produced in the first stage, can be stored immediately in the memory space containing the odd samples of the input data because these odd samples are not

Fig. 5 The architecture of 9/7 1D-DWT based on LS



used in later stages of computation. Similarly the results produced in the second stage can be stored back to the memory space allocated to the even samples of input data. Continuing in the same way, the high-pass ($P_2 : H_k = x'_{(2k+1)_{new}} + c \cdot (x_{((2k)_{new})_{left}} + x_{((2k)_{new})_{right}})$) and the low-pass ($U_2 : L_k = x'_{(2k)_{new}} + d \cdot (H_{k-1} + H_k)$) output samples are stored into the registers where the odd (even) samples of the input data were originally stored at the beginning of the computation. As a result, no extra memory is required at any stage. For each sample pixel, low-pass decomposition requires 8 shifts (S) and 8 additions (A) instructions whereas high-pass decomposition requires 2 shifts and 4 additions. The energy needed for low-pass/high-pass decompositions may be defined by the number of operations. This energy called “computational load”. Therefore the low-pass decomposition requires $8S + 8A$ units of computational load in a unit pixel and $2S + 4A$ units for the high-passes. At a transform level, each pixel is read and written twice. We estimate that the “data-access load” is the number of read and write operations. Assuming that the input image size is of $M \times N$ pixels and that the image is decomposed into p resolution level, then the 2D-DWT is iteratively applied $p - 1$ levels. Since the image is divided into 4 sub-bands in each transform level, the total computational energy for this process can be computed as a sum of the computational load and data-access load as follows:

$$E_{DWT}(M, N, p) = MN(10S + 12A + 2R_{mem} + 2W_{mem}) \cdot \sum_{i=1}^{p-1} \left(\frac{1}{4}\right)^{i-1} = \frac{4}{3}MN(10S + 12A + 2R_{mem} + 2W_{mem}) \left[1 - 4^{-(p-1)}\right] \quad (3)$$

In this study, we have adopted the parameters which refer to the characteristics of MICA2 motes, where, S , A , R_{mem} , and W_{mem} represent the energy consumption for shift, add, read, and write basic 1-byte instructions, respectively [Atmel Corporation \(2006\)](#).

The energy spent in entropy coding per bit is

$$E_{ENT} = \delta. \quad (4)$$

The value of the parameter of the computation energy model (6) is estimated as follows. We have employed Joule-Track [Sinha and Chandrakasan \(2001\)](#) to estimate the energy consumption for an existing JPEG2000 coder [Adams \(2003\)](#). From the experiment, the value of δ is estimated to be 20×10^{-9} J/bit.

To estimate the communication energy, the transceiver energy dissipation model is used. The energy consumed in reception per bit is

$$E_{RX} = \varepsilon_e \quad (5)$$

The energy consumed in transmission one bit is

$$E_{TX} = \varepsilon_e + \varepsilon_a d^\alpha \quad (6)$$

where, ε_e is the energy consumed by the circuit per bit, ε_a is the energy dissipated per bit per m^2 , d is the distance between a wireless transmitter and a receiver, and α is an attenuation factor depending on the environment with typical values between 2 and 6. The parameter value for wireless communication energy model (4) and (5) are the typical values $\varepsilon_a = 100 \times 10^{-12}$, $\varepsilon_e = 50 \times 10^{-9}$ as for example in [Heinzelman et al. \(2000\)](#) and α is chosen 2.

To analyze the degradation of image quality, we shall use the PSNR metric, which is defined (in decibels) as:

$$PSNR = 10 \log_{10} \frac{(2^q - 1)^2}{MSE} \quad (7)$$

where q is the number of bits per pixel (bpp) of the raw image, and MSE is the mean-square-error which defined by:

$$MSE = \frac{1}{MN} \sum_{m=0}^{M-1} \sum_{n=0}^{N-1} [i(m, n) - \hat{i}(m, n)]^2 \quad (8)$$

where $i(m, n)$ is the pixel values of the original image, $\hat{i}(m, n)$ is the pixel values reconstructed image.

3.3 Distributed task of the image compression

The basic idea of the proposed distributed image compression is distributing the workload of task to several groups of nodes along the path from the source to the sink. The key issue in the design of distributed task of image compression is data exchange. In this proposition, data is broadcasted to all processors to speed up the execution time which may optimize network lifetime and increase the energy consumption. We proposed two data exchange schemes based on distributed cluster-based compression and compare between them with respect to image quality and energy consumption; (1) Method 1 based on the standard LS 9/7 DWT; (2) Method 2 based on the elimination of insignificant wavelet coefficients. In this study, the network is grouped into different clusters. Each cluster is composed of one cluster head and many cluster member nodes. The cluster head can process, select and aggregate sensed data from cluster member nodes.

3.3.1 Method 1

In this method, we consider the data partitioning scheme proposed using the LS 9/7 DWT. An example of distributed cluster-based compression using four nodes in each cluster is shown in Fig. 7. A routing algorithm is assumed to be in place and nodes are self-organized into a two-tiered architecture [Krishnan and Starobinski \(2006\)](#).

When applying the scenario proposed in Sect. 4 and after receiving a query from a source node s , the cluster head c_1 selects a set of nodes n_{1i} ($i = 1 \dots 4$) in the cluster which will take part in the distributed tasks then informs source node. The source divides the original image into tile and transmits them to n_{1i} (n_{11}, n_{12}, n_{13} and n_{14}). Those nodes run 1D-DWT (horizontal decomposition) on their received data then send the intermediate results to c_2 . After receiving the results, c_2 distributes it to the set of nodes n_{2i} (n_{21}, n_{22}, n_{23} and n_{24}). These nodes process data (vertical decomposition) and send the results (Level 1 data in Fig. 5b) to the next cluster head c_3 . The cluster head c_3 chooses a part of the results (corresponding to LL_1 in Fig. 5b) and distributes it to the set of nodes n_{3i} . Those nodes run 1D wavelet transform algorithm of LL_1 sub-band then send the intermediate results to c_4 . The remaining part of the image (HL_1, LH_1 and HH_1 in Fig. 5b) is coded and sent to the next cluster head c_4 . Without combining process, the cluster head c_4 forwards the results corresponding to L_2 and H_2 sub-bands directly to the set of nodes n_{4i} (n_{41}, n_{42}, n_{43} and n_{44}). These nodes send their processed results (LL_2, HL_2, LH_2 and HH_2 in Fig. 5c) to c_5 after running a second 1D-DWT (vertical decomposition). The remaining sub-bands (HL_1, LH_1 and HH_1 in Fig. 5b) is coded and sent also to the next cluster head c_5 . To be compatible with experiment results and depending on the image quality specified by the query (which is application-dependent), this procedure may continue on c_6 and its following nodes until the final compressed image reaches the destination node. It should be noted that, as shown in Fig. 6, after the DWT, all the sub-bands are quantized by a single node (n_{5i}). The other nodes are put awake. Since the quantization represents about 5.5 % of the total process time, In spite of resource constraints, an individual node has a sufficient power to realize the quantization block. Given that the Tier-1 coding represents about 43 % of the total process time, the tasks partition-

ing optimize the network lifetime. After receiving the results, c_6 divides quantized sub-bands into a number of smaller code-blocks of equal size and send their processed results to set of nodes n_{6i} (n_{61}, n_{62}, n_{63} and n_{64}). In these nodes each code-block is entropy encoded independently to produce compressed bit-streams.

3.3.2 Method 2

The basic idea of the proposed technique is avoiding the computation of insignificant coefficients during the transform step. This technique attempts to conserve energy by skipping the least significant sub-band. Thus, the proposal reduces the number of arithmetic operations and memory accesses. The proposed technique is called “*EHPF: Elimination High Pass Filtering*”. Figure 7 illustrates the distribution of high-pass coefficients after applying tow levels wavelet transform to the 256×256 image. We notice that the high-pass coefficients values are very small. Indeed, 75 % of the high pass coefficients for level 1 are less than 5.

This explains that the LPF can compact the significant coefficients in the LL_i sub-band. Thus, the most of the image energy is located in L_i sub-band also during the horizontal decomposition. Therefore, in the vertical direction only the LPF is applied in each compression level resulting in a minimum image quality loss. The sub-bands resulting from the horizontal direction are further decomposed in the vertical direction applying only the LPF, leading to LL_1 and HL_1 sub-bands. The other high-pass sub-bands (LH_i , and HH_i) are removed. After one transform level, the image is then processed by applying the 2-D sub-band decomposition to the LL_i sub-band while applying only the LPF in the vertical direction. This process can be repeated up to any level.

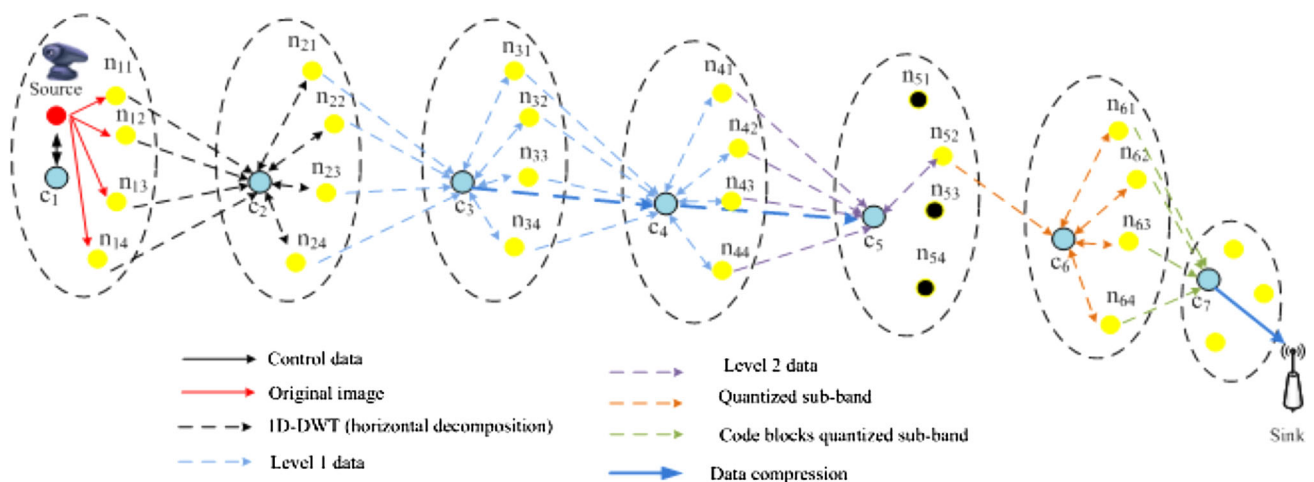


Fig. 6 Data exchange of distributed task for image compression in a multi-hop wireless network. Two levels of wavelet decomposition are used

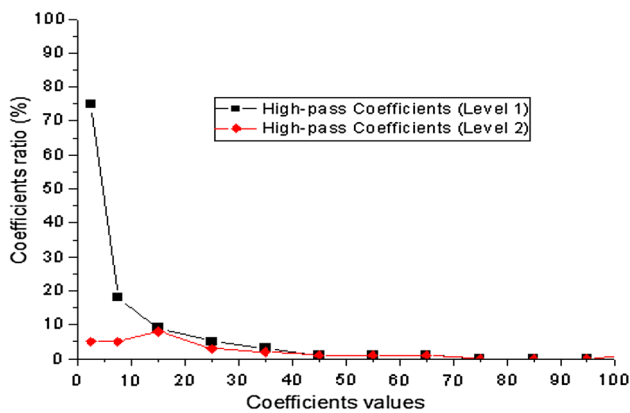


Fig. 7 Distribution of high-pass coefficients

Similar to method 1, after receiving a query from a source node s , the cluster head c_1 selects a set of nodes n_{1i} ($i = 1 \dots 4$) in the cluster which will take part in the distributed tasks then informs source node. The source divides the original image into tile and transmits them to n_{1i} (n_{11}, n_{12}, n_{13} and n_{14}). Those nodes run 1D-DWT (horizontal decomposition) on their received data then send the intermediate results to c_2 . The cluster head c_2 sends the received data to the processing nodes n_{2i} (n_{21}, n_{22}, n_{23} and n_{24}) to run 2-D DWT. In this decomposition, both sub-bands (L_1 and H_1) resulting from the horizontal direction are only fed into the LPF and not the HPF in the column transform step. After running a second 1D-DWT (vertical decomposition), the set of nodes n_{2i} send their processed results (LL_1 and HL_1 in) to c_3 . The cluster head c_3 selects a part of LL_1 sub-band and forwards it to the set of nodes n_{3i} (n_{31}, n_{32}, n_{33} and n_{34}). Those nodes run the 1D-DWT (horizontal decomposition) on their received data then send the results individually to c_4 . The remaining part of the image (HL_1 sub-band) is coded and sent to the next cluster head c_4 . Similar to method 1 implementation, this procedure may repeat several times until the requested compression level is satisfied. Then, the transformed coefficients are quantized by an individual node in order to reduce the volume of encoded data. Following the quantization step, an encoding module provides a sequence of binary symbols similar to method 1.

3.4 Network density versus requested parameters

In the proposed distributed scheme, the requested parameters may be obtained when reaching a same processing level, depending on the wireless applications. In each cluster head, data processing is made to select the next hop. In this case, the respective cluster head compares calculated parameters with those memorized in each node during the transmission request process as explained in Sect. 4. Depending on the result of the comparison:

- (i) If the requested parameters are fulfilled, the cluster head directly forwards the processed data to the next cluster head without further processing, and then from cluster head to the next cluster head until it reaches the sink.
- (ii) If the requested parameters are not fulfilled yet, the cluster head will process data then forwards them to its cluster member nodes for further data processing. This process is repeated several times until the requested QoS is satisfied.
- (iii) If the sink asks for a very good QoS with high PSNR, and we will not be able to get the required quality needed by the sink, the respective cluster head sends a message to the sink to inform that this application is infeasible.

Then remains the question: How about the situations in case the distance between the source and the sink is not large enough? In this study, the last cluster member nodes on the path to the sink may have to perform multiple operations on the remaining data until the requested parameters is reached. We call this the '*last-cluster overload*'. This may potentially induce a fast depletion of the nodes located next to the sink. In view of this, after processing data in the current cluster head, the proposed state transition adopts the approach of the compression data is described in Fig. 8.

For example, if the source is four hops away from the sink while the required compression level is two, the relaying nodes n_{4i} will compute the remaining processing data. Indeed, after running the vertical decomposition, the set of nodes n_{4i} send the results to c_4 . The cluster head c_4 send the processed data again to one of the processing nodes (n_{4i}) to realize the quantization block. These nodes process data and send the results to the cluster head c_4 . After receiving the results, c_4 divides quantized sub-bands into a number of smaller code-blocks of equal size and forwards their processed results to set of nodes n_{4i} . In these nodes each code-block is entropy encoded independently to provide a sequence of binary symbols.

For the set of member nodes which located next to the sink, the data is in a more compressed form than those towards the source; therefore, the energy cost of these nodes is smaller than the energy cost of previous processing nodes on the path. For the reason the '*last-cluster overload*' will not have a significant effect on the system lifetime.

4 Results and discussions

In this section, we analyze the functional influence of the parameters initialized in the scenario proposed in QoSs requirements. Then, we study the impact of some parameters on the behavior of the distributed schemes to evaluate energy performance of image transmission. However, the variation

Fig. 8 Proposed transition state of the data compression at an intermediate cluster head

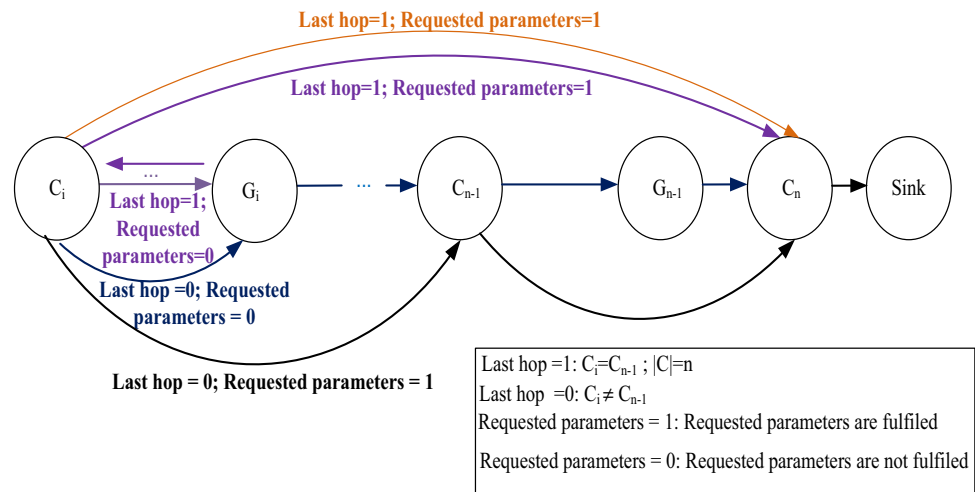
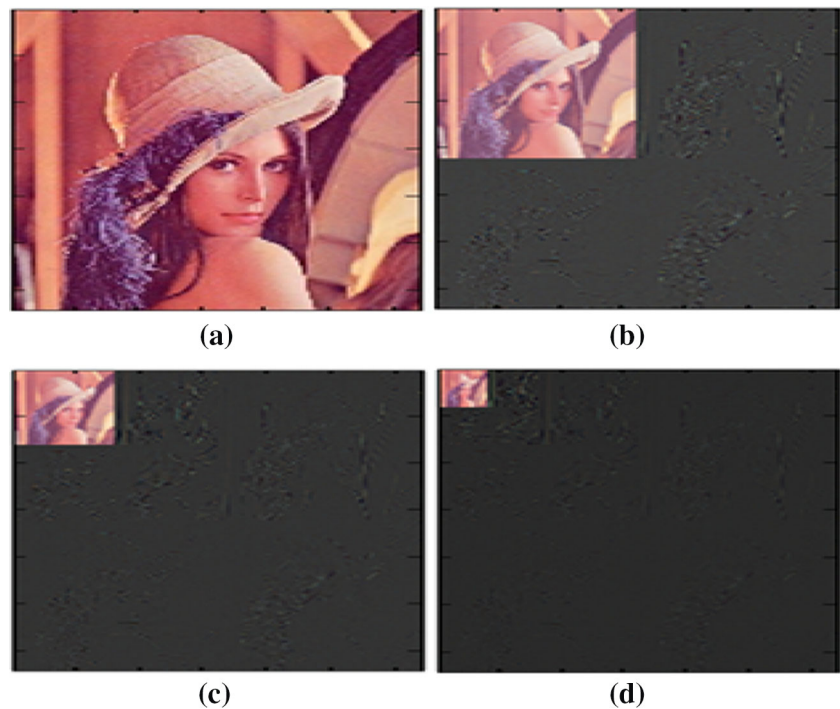


Fig. 9 **a** Original image component. **b** Output image after the first decomposition level. **c** Output image after the second decomposition level. **d** Output image after the third decomposition level



of these parameters to ensure a multi-level processing should affect other interesting factors which may influence the communication process quality such as:

- Execution time on the microcontroller (sensor node)
- PSNR

4.1 Impact of the DWT on computational energy

In this section, we report on computation energy consumed and generated by each of the two proposed techniques as described in the previous section. To implement the method 1, the energy localization by successive decomposition lev-

els will allow decreasing the amount of information to be transmitted to the destination. The computed quantity is divided by 4 at every decomposition level as shown in Fig. 9. This is a main objective to be achieved, since the energy consumption in sensor nodes is proportional to the information quantity being transmitted over the wireless channel.

As a result, reducing the quantity of transmitted data will extend the topological lifetime of WSNs. From the experiment, a Lena image of 256×256 pixels is used as a test image. We first apply the decomposition in the horizontal direction. Since all even-positioned image pixels are decomposed into the low-pass coefficients and odd positioned image pixels are

decomposed into the high-pass coefficients, the total computational energy involved in horizontal decomposition is given as.

$$E_H(M, N) = \frac{1}{2}MN(10S + 12A + 2R_{mem} + 2W_{mem}) \quad (9)$$

The energy consumed by each node n_{1i} and n_{2i} ($i = 1, \dots, 4$) to run 1D-DWT is of about 301 mJ (by component) respectively and 75 mJ to run 1D wavelet transform algorithm of LL_1 sub-band (n_{3i} and n_{4i}) corresponding to a 75 % drop off.

While the method 1 reduces some computation loads during the transform steps, the method 2 targets more significant computation energy savings. The energy consumed in the horizontal decomposition, is similar to the method 1. However, during the column transform the high-pass sub-band (HH_1) and (LH_1) are not computed, resulting in less computed operation and hence saving computational load. The computation load saving is given by:

$$\begin{aligned} & \underbrace{\frac{1}{4}MN \cdot (4A + 2S)}_{LH} + \underbrace{\frac{1}{4}MN \cdot (4A + 2S)}_{HH} \\ &= \frac{1}{2}MN \cdot (4A + 2S) \text{ (13.7 \% compared to the LS 9/7).} \end{aligned}$$

In this study, we assume that the method 1 technique is applied to the first E transform levels out of the $(p - 1)$ total transform levels Nasri et al. (2011). This is because the advantage of skipping high-pass coefficients is more significant at lower transform levels. Therefore, the total computational load using this technique is represented as:

- Computational load:

$$\begin{aligned} C_{EHPF} &= MN(10A + 9S) \sum_{i=1}^E \left(\frac{1}{4}\right)^{i-1} \\ &+ MN(10A + 9S) \sum_{i=E+1}^{p-1} \left(\frac{1}{4}\right)^{i-1} \\ &= MN(10A + 9S) \sum_{i=0}^{E-1} \left(\frac{1}{4}\right)^i \\ &+ MN(10A + 9S) \sum_{i=E+1}^{p-2} \left(\frac{1}{4}\right)^i \\ &= MN(12A + 10S) \sum_{i=0}^{E-1} \left(\frac{1}{4}\right)^i \\ &+ MN(10A + 9S) \sum_{i=E+1}^{p-2} \left(\frac{1}{4}\right)^i \\ &- MN(2A + S) \sum_{i=0}^{E-1} \left(\frac{1}{4}\right)^i \end{aligned}$$

$$\begin{aligned} &= \frac{4}{3}MN(12A + 10S) \left[1 - 4^{-(p-1)}\right] \\ &- \frac{4}{3}MN(2A + S) \left[1 - 4^{-E}\right] \end{aligned} \quad (10)$$

From Eqs. (3) and (10), we have determined the total gain which is defined by :

$$\begin{aligned} Gain &= \frac{4}{3}MN(12A + 10S) \left[1 - 4^{-(p-1)}\right] \\ &- \frac{4}{3}MN(12A + 10S) \left[1 - 4^{-(p-1)}\right] \\ &+ \frac{4}{3}MN(2A + S) \left[1 - 4^{-E}\right] \\ &= \frac{4}{3}MN(2A + S) \left[1 - 4^{-E}\right] \end{aligned} \quad (11)$$

On the other hand, the reduced computed operation induces less memory access operation. Therefore, one can save on a half of “write” operations during the column transform compared to the method 1 corresponding to $\frac{1}{2}MN(R_{mem} + R_{mem})$ of data-access load. Therefore, the method 1 reduces some data-access loads during the transform steps by skipping two out of every four sub-bands. The total data-access load is given by:

- Data-access load:

$$\begin{aligned} C_{Read-LS9/7} &= C_{Read-EHPF} \\ C_{Write-EHPF} &= \frac{3}{2}MNW_{mem} \sum_{i=0}^{E-1} \left(\frac{1}{4}\right)^{i-1} \\ &+ 2MNW_{mem} \sum_{i=E}^{p-2} \left(\frac{1}{4}\right)^{i-1} \\ &= 2MNW_{mem}(1 - 4^{-(p-1)}) \end{aligned} \quad (12)$$

The average energy dissipated by every node using the proposed methods is provided in Fig. 10.

In this case, we were interested by analyzing the impact of the decomposition levels on the enhancement of the execution time. Figure 11 represents the execution time till five decomposition levels.

We have considered Lena image with different sizes. The process time vary over decomposition levels and then reduced and become almost constant from the third decomposition level. Thus, the most of the image energy is located in LL_i sub-band. Therefore, an additional decomposition level is useless and will waste energy without extracting more details. This shows that the required number of wavelet decomposition levels in practice is typically small. Most image-based applications consist of a large number of wireless sensor nodes and the source is at least eight hops away from the sink. Thus, at least eight clusters are used. For the reasons above, the sensor nodes located next to the sink are

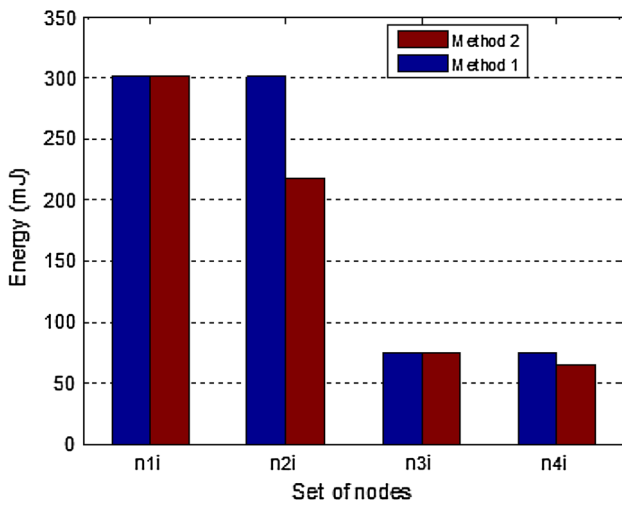


Fig. 10 Computational energy dissipated by every set of nodes

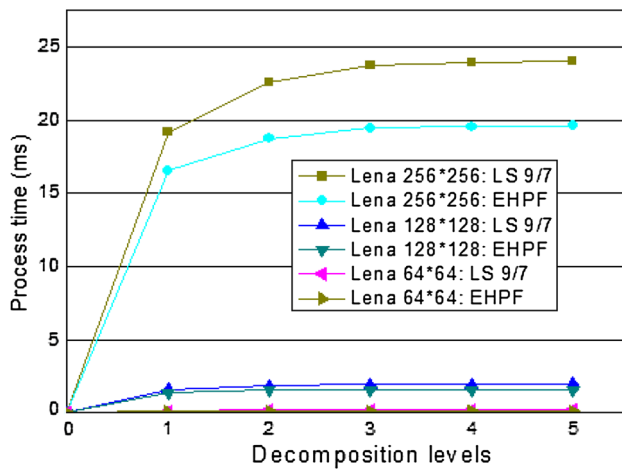


Fig. 11 Processing time for five decomposition levels

less likely to be overburdened with computational requirements.

4.2 Impact of the entropy encoding

Coding a 32×32 LL sub-band (decomposition level = 3) with 4 magnitude bit planes, the energy dissipated is of about $5 \mu\text{J}$ (pass1) and $15 \mu\text{J}$ (pass 2), whereas energy dissipated by the pass3 is inconsiderable. For a 32×32 LL sub-band with 5 magnitude bit planes, the average energy dissipated to run pass1 and pass2 is estimated to be $10 \mu\text{J}$ each and the energy spent in pass3 is of about $2 \mu\text{J}$. Therefore, decrease in magnitude bit planes leads to lower image quality (Table 1) and less computation energy. We have also studied the image transfer adaptability to WSNs through the analysis of some image compression parameters. This study has been achieved by analyzing the dependence between system lifetime and allocated memory, and helped to select the better compression rate as well as the better image quality.

The most important data are provided in the Table 1. Despite, the better image quality provided by method 1, the result of the method 2 processing is still acceptable in WSNs applications for the highest bit plane.

5 Conclusion

In this paper, we have proposed and analyzed a new energy efficient image compression and transmission scheme for wireless sensor networks. This scheme is based on wavelet image compression to reduce both computation energy by reducing the number of arithmetic operations and memory accesses as well as communication energy by reducing the number of transmitted bits. This technique presents a poten-

Table 1 Measure basic elements

	Method 1			Method 2		
	PSNR	Execution time	Class of service	PSNR	Execution time	Class of service
DWT decomposition level = 3 and Number of bit plane = 4	20.92	Low	Low image quality with low response time	18.49	Low	Low image quality with very low response time
DWT decomposition level = 3 and Number of bit plane = 5	27.34	Average	Average image quality with average response time	24.62	Low	Low image quality with average response time
DWT decomposition level = 3 and Number of bit plane = 6	31.16	High	Average image quality with a high response time	26.36	Average	Average image quality with average response time
DWT decomposition level = 3 and Number of bit plane = 7	33.5	High	Acceptable image quality with a high response time	29.68	High	Still acceptable image quality with high response time

tial solution to the emerging problems related to image transmission in wireless applications.

This work offers much flexibility at different process levels. These flexibilities are considered as dynamic parameters during the system to adapt the communication process. We have focused our study on the design and evaluation of an efficient image compression depending on the operating parameters at different process levels. Performance evaluation shows that the proposed scheme should minimize communication energy which is proportional to the number of transmitted bits and therefore, extends the overall network lifetime.

In future work it is reasonable to validate our approach using a real platform to satisfy the real time constraints.

References

- Adams, M.D. (2003). The JasPer project home page. <http://www.ece.uvic.ca/mdadams/jasper/>.
- Atmel Corporation. (2006). Atmega128L microcontroller datasheet, Technical report.
- Boulgouris, N., & Strintzis, M. (2002). A family of wavelet-based stereo image coders. *IEEE Transactions on Circuits and Systems for Video Technology Journal*, 12(10), 203–898.
- Ferrigno, L., Marano, S., Paciello, V., & Pietrosanto A. (2005). Balancing computational and transmission power consumption in wireless image sensor networks. In *Proceedings of international conference on Virtual Environments, Human-Computer Interfaces, and Measures Systems (VECIMS'05)* (pp. 61–66). Giardini Naxos.
- Flammini, A., Ferrari, P., Marioli, D., Sisinni, E., & Taroni, A. (2009). Wired and wireless sensor networks for industrial applications. *Microelectronics Journal*, 40(9), 1322–1336.
- Heinzelman, W.R., Chandrakasan, A., & Balakrishnan, H. (2000). Energy-efficient communication protocol for wireless microsensor networks. In *Proceedings of Hawaii International Conference on System Sciences* (pp. 1–10). Washington.
- Heinzelman, W.R., Chandrakasan, A., & Balakrishnan, H. (2000). Energy-efficient communication protocol for wireless microsensor networks. In *Proceedings of the Hawaii International Conference on System Science (HICSS)* (pp. 3005–3014). Hawaii.
- Heinzelman, W.R., Kulik, J., & Balakrishnan, H. (1999). Adaptive protocols for information dissemination in wireless sensor networks. In: *Proceedings of ACM/IEEE Mobile computing and networking* (pp. 174–185). Seattle, Washington, DC.
- Jeon, H., Park, K., Hwang, D. J., & Choo, H. (2009). Sink-oriented dynamic location service protocol for mobile sinks with an energy efficient grid-based approach. *MDPI Sensors*, 9(3), 1433–1453.
- Krishnan, R., & Starobinski, D. (2006). Efficient clustering algorithms for self organizing wireless sensor networks. *Ad Hoc Networks Journal*, 4(1), 36–59.
- Liu, M., Cao, J., Chen, G., & Wang, X. (2009). An energy-aware routing protocol in wireless sensor networks. *MDPI Sensors*, 9(1), 445–462.
- Lu, Q., Luo, W., Wanga, J., & Chen, B. (2008). Low-complexity and energy efficient image compression scheme for wireless sensor networks. *Computer Networks Journal*, 52(13), 2594–2603.
- Mohamed El-Semary, A., & Mostafa Abdel-Azim, M. (2013). New trends in secure routing protocols for wireless sensor networks. *International Journal of Distributed Sensor Networks*, 2013, ID 802526.
- Muthuramalingam, S., Malarvizhi, R., Veerayazhmi, R., & Rajaram, R. (2008). Reducing the cluster overhead by selecting optimal and stable cluster head through genetic algorithm. In *Proceedings of IEEE Asia International Conference on Modeling & Simulation* (pp. 540–545). Kuala Lumpur.
- Nasri, M., Helali, A., Sghaier, H., & Maaref, H. (2011). Adaptive image compression technique for wireless sensor networks. *Computers & Electrical Engineering*, 7(5), 798–810.
- Park, S., Shin, K., Abraham, A., & Han, S. (2007). Optimized self organized sensor networks. *Sensor*, 7(5), 730–742.
- Sinha, A., & Chandrakasan, A. (2001). JouleTrack-a web based tool for software energy profiling, Design Automation Conference (pp. 220–225). <http://www-ml.mit.edu/research/anantha/jouletrack/JouleTrack/index.html>.
- Wagner, R., Nowak, R., & Baraniuk R. (2003). Distributed image compression for sensor networks using correspondence analysis and super-resolution. In *Proceedings of IEEE International Conference on Image Processing (ICIP'03)* (pp. 597–600). Boston: Kluwer Academic.
- Wu, H., & Abouzeid A.A. (2004). Energy efficient distributed JPEG2000 image compression in multihop wireless networks. *4th Workshop on Applications and Services in Wireless Networks (ASWN'04)* (pp. 152–160). Boston.
- Wu, M., & Chen C.W. (2005). Multiple bitstream image transmission over wireless sensor networks. In *Proceedings of IEEE Sensors* (pp. 727–731). Toronto.
- Wu, H., & Abouzeid, A. A. (2005). Energy efficient distributed image compression in resource-constrained multihop wireless networks. *Computer Communication Journal*, 28(14), 1658–1668.